International Symposium
On Turbulence and Shear Flow
Phenomena (TSFP-8)
August 28 - 30, 2013 Poitiers, France

ODTLES SIMULATIONS OF TURBULENT FLOWS THROUGH HEATED CHANNELS AND DUCTS

Christoph Glawe
BTU Cottbus
Siemens-Halske-Ring 14, 03046 Cottbus, Germany
Christoph.Glawe@tu-Cottbus.de

Falko T. Schulz
BTU Cottbus
Siemens-Halske-Ring 14, 03046 Cottbus, Germany
schulzf@tu-Cottbus.de

Esteban D. Gonzalez-Juez
Combustion Science & Engineering, Inc.
Columbia, MD 21045, USA
estebandgj@gmail.com

Heiko Schmidt
BTU Cottbus
Siemens-Halske-Ring 14, 03046 Cottbus, Germany
schmidth@tu-Cottbus.de

Alan R. Kerstein
Consultant
72 Lomitas Road, Danville, CA 94526, USA
alan.kerstein@gmail.com

ABSTRACT

A widely occurring problem in fluid dynamics either in engineering or e.g. hydrology is the turbulent transport through channels and ducts. ODTLES, a stochastic based multi-scale and multi-dimensional model, is a promising tool to describe these flows even including scalar properties like temperature. We are quantifying the ability of ODTLES to describe the heated channel flow with respect to the Prandtl number and the flow through squared ducts with respect to the Reynolds number.

INTRODUCTION

An interesting challenge in classical mechanics is the description of a turbulent fluid. A key difficulty in modelling these flows is their multi-scale nature. Even fundamental problems like the flow through a channel or duct are still under study and have been investigated by several groups in experiments (e.g. Hirota *et al.* (1997)) and numerical studies (e.g. Kawamura *et al.* (1999), Pinelli *et al.* (2010)). Direct Numerical Simulations (DNSs) are widely used to investigate these fundamental problems because they are solving the governing physical incompressible Navier-Stokes equations without assumptions. So DNSs can yield the complex statistics of moderate Reynolds number channel and duct flows, but are limited mostly to fundamental research due to the wide range of spatial and temporal scales emerging in technical and meteorological flows. These problems are for example treated by modeling small scales in Large-Eddy-Simulations (LES). These models have issues in resolving non-isotropic flow regions (e.g. near wall and stratified flows) and turbulent backscatter effects. The disagreement in the scientific community about the influence of the latter effects (e.g. Piomelli *et al.* (1991)) indicates the lack of understanding.

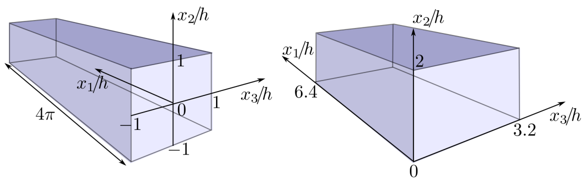

Figure 1. Coordinate system and geometry of the duct (left) and the channel (right).

From this point of view, stochastic approaches based on One-Dimensional-Turbulence (ODT) (e.g. Kerstein *et al.* (2001), Kerstein (1999)) and multi-dimensional approaches incorporating ODT, like ODTLES (e.g. Schmidt *et al.* (2008) and Gonzalez-Juez *et al.* (2011)), are an interesting alternative. The ability of ODT to resolve molecular effects (as DNSs) and to describe even non isotropic 3D turbulence using a stochastic process distinguishes ODT and ODTLES from techniques such as LES and Reynolds-Averaged-Navier-Stokes (RANS) models.

NUMERICAL METHODOLOGY

We are considering incompressible flows in a channel and a duct (see fig. 1). The square duct is bounded by walls at the faces normal to $x_3 = \{-h,h\}$ and $x_2 = \{-h,h\}$, the channel by walls at $x_2 = \{0,2h\}$. All other boundary conditions are considered periodic to mimic e.g. an infinite streamwise extension in the x_1-direction. The turbulent channel can be described by both ODT and ODTLES, the square duct only by ODTLES due to the three dimensional non turbulent properties (e.g. secondary instabilities) of the characteristic flow. To understand the approach of ODTLES, a brief description of ODT will follow first.

Table 1. Nomenclature

ν	kinematic viscosity
κ	thermal diffusivity
ρ	density of the fluid
h	Spatial scale (e.g. channel half width)
Ω	comput. domain
$\Phi = \partial_{x_1} p$	mean pressure gradient
$\overline{(\ )}$	time averaged quantity
$(\ )^{RMS}$	root mean square
$\langle\ \rangle_{x_k}$	in x_k-direction averaged quantity
τ_W	wall shear stress
$u_\tau = \sqrt{\tau_W/\rho}$	friction velocity
$Re_\tau = u_\tau h/\nu$	Reynolds number
$u_B = \int_\Omega u\,\mathrm{d}V$	bulk velocity
$Re_B = u_B h/\nu$	Reynolds number

One-Dimensional-Turbulence Model

For a detailed introduction see the publications of Kerstein (1999) and Kerstein *et al.* (2001) and for the scalar extension we refer to Wunsch & Kerstein (2000), Ashurst & Kerstein (2005), and Schmidt *et al.* (2012). ODT emulates the time evolution of a turbulent 3D fluid in a 1D subspace w.l.o.g. in the x_2-direction (used in the channel case). The time evolution of a velocity vector $\mathbf{u} = (u_1, u_2, u_3)$ along the directions (x_1, x_2, x_3) and a scalar θ are described by

$$\begin{aligned}\partial_t \mathbf{u}(\mathbf{x_2};\mathbf{t}) + e_{\mathbf{u}}(\mathbf{u}(x_2;t), y_0, l) &= \nu \partial_{x_2}^2 \mathbf{u}(x_2;t) - \Phi/\rho \qquad (1)\\ \partial_t \theta(x_2;t) + e_\theta(\theta(x_2;t), y_0, l) &= \kappa \partial_{x_2}^2 \theta(x_2;t) - F_{\mathbf{u}\to\theta}(u_2(x_2;t))\end{aligned}$$

where $F_{\mathbf{u}\to\theta}(u_2)$ is a problem dependent coupling term and $\{e_{\mathbf{u}}(\mathbf{u}), e_\theta(\theta)\}$ is an instantaneous eddy function affecting $\{\mathbf{u}, \theta\}$ within the eddy range $x_2 = [y_0, y_0 + l]$. This eddy function is introduced to represent the stochastic procedure appearing like turbulent advection:

$$\begin{aligned} e_{\mathbf{u}} &: \mathbf{u}(x_2,t) \to \mathbf{u}(f(x_2),t) + \mathbf{c}K(x_2) \qquad (2)\\ e_\theta &: \theta(x_2,t) \to \theta(f(x_2),t)\end{aligned}$$

Here K is a kernel function which in combination with $\mathbf{c}$ assures energy conservation and controls the energy redistribution among the velocity components (for details see Kerstein *et al.* (2001)). The mapping function $f(x_2)$, representing the fluid transport, is measure preserving, continuous and satisfies the requirement of scale locality. These indispensable physical requirements for $f(x_2)$ are satisfied by a triplet map, which places three compressed copies of the original $\{\mathbf{u}(x_2), \theta(x_2); x_2 \in [y_0, y_0 + l]\}$ profile in the eddy range and reverses the middle copy to preserve continuity:

$$f(x_2) = y_0 + \begin{cases} 3(x_2 - y_0), & \text{if } y_0 \le x_2 \le y_0 + \frac{1}{3}l \\ 2l - 3(x_2 - y_0), & \text{if } y_0 + \frac{1}{3}l \le x_2 \le y_0 + \frac{2}{3}l \\ 3(x_2 - y_0) - 2l, & \text{if } y_0 + \frac{2}{3}l \le x_2 \le y_0 + l \\ (x_2 - y_0), & \text{else} \end{cases} \qquad (3)$$

To insert the eddy function $\{e_{\mathbf{u}}(\mathbf{u}), e_\theta(\theta)\}$ into the time evolution equation (1), the eddy size l and the location y_0 are sampled from a probability distribution representing the physics. For given $\{l, y_0\}$ an eddy turnover time can be calculated leading to an occurrence frequency $\frac{1}{\tau}$. Since the ODT triplet map is an instantaneous process, the frequency for the eddy specified by $\{l, y_0\}$ is chosen from an event rate distribution:

$$\lambda(y_0, l) = \frac{C}{l^2 \tau(y_0, l)} = \frac{C}{l^4}\sqrt{E_{kin} - E_{pot} - Z} \qquad (4)$$

involving particular definitions of the kinetic energy E_{kin} and the potential energy E_{pot}, which vanishes in the current cases. The values C and Z are model adjustable parameters. The latter is introduced to cut off eddies with unphysically small energy and the parameter C is an overall rate coefficient determining the strength of the turbulence.

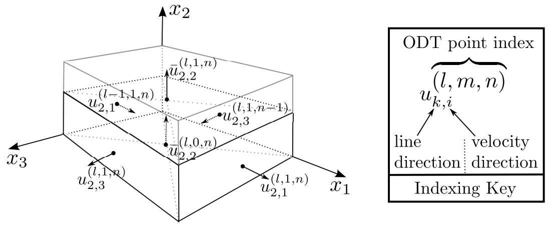

Figure 3. Illustration of the velocities located on the faces (staggered grid) of an ODT wafer for an ODT line in the x_2-direction. An ODT j-index of zero denotes the lower boundary of the computational domain. A unit increment of j corresponds to the ODT-scale while unit increments of i and k correspond to the LES-scale.

ODTLES

A scalar extension of ODTLES using a passive scalar is introduced in this section. For a detailed introduction to a non-scalar ODTLES model see the publications of Schmidt *et al.* (2008) and Gonzalez-Juez *et al.* (2011).

In ODTLES the 3D computational domain is divided into coarse LES-like 3D control volumes (see fig. 2 (a)) and three coupled and orthogonal sets of ODT lines each defining a nominally space-filling 3D ODT line domain (see fig. 2 (b)-(d)). Since ODTLES is developed as a spatial and temporal multi-scale approach the governing equations split into the ones solved on the LES-scale and those solved on the ODT-scale. $\{\Delta T, \Delta X, \partial_T, \partial_X\}$ denotes the LES-scale temporal (based on a CFL condition) and spatial increments and their partial derivatives while $\{\Delta t, \Delta x, \partial_t, \partial_x\}$ corresponds to the ODT-scale counterparts. The ODT-scale fluxes can be divided into the one used in the ODT scheme (compare eq. (5) with eq. (1)) and the advective fluxes in the ODT line direction (on a timescale $\Delta t_{adv} \approx \Delta t$).

On the ODT line domains we solve for each direction x_k with $k = \{1, 2, 3\}$ (please note the index key in fig. 3) for

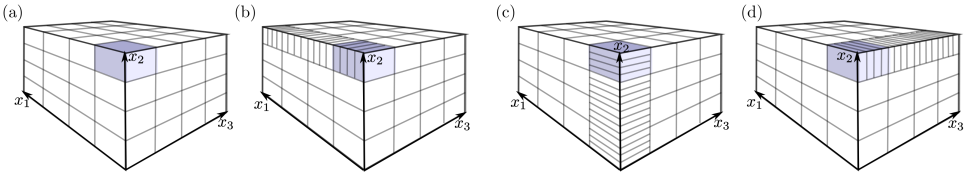

Figure 2. An ODTLES domain Ω is divided into a 3D control volumes (a), with N^3_{LES} so called LES cells (see blue cell; here, $N_{LES}=4$), and nominally 3D ODT domains containing (operationally 1D) ODT lines in x_1-direction (b), x_2-direction (c) and x_3-direction (d). Each subfigure (b) - (d) shows one characteristic ODT line divided into $N_{ODT}=16$ wafers. Parts of ODT lines in each direction are intersecting a LES cell (e.g. blue cell)

the velocities

$$\begin{aligned}\int_t^{t+\Delta T} \partial_{t'} u_{k,i}\,\mathrm{d}t' = & \qquad (5)\\ & \sum_{n=1}^{\Delta T/\Delta t}\left(\int_{t+(n-1)\Delta t}^{t+n\Delta t}\left[-e_{\mathbf{u}}(\mathbf{u}_k,y_0,l)+\nu\partial^2_{x_k}u_{k,i}-\Phi/\rho\right]\mathrm{d}t'\right)\\ + & \sum_{n=1}^{\Delta T/\Delta t_{adv}}\left(\int_{t+(n-1)\Delta t_{adv}}^{t+n\Delta t_{adv}}\left[-\partial_{x_k}(\bar{u}_{k,k}u_{k,i})\right]\mathrm{d}t'\right)\\ + & \int_t^{t+\Delta T}\Big[-\partial_{X_i}(\bar{u}_{k,i}u_{k,i})-\partial_{X_j}(\bar{u}_{k,j}u_{k,i})\\ & \qquad -\partial_{X_i}\bar{P}/\rho+\partial_{X_i}\left(\nu\partial_{X_i}u_{k,i}\right)+\partial_{X_j}\left(\nu\partial_{x_j}u_{j,i}\right)\Big]\mathrm{d}t'\end{aligned}$$

and for the scalar

$$\begin{aligned}\int_t^{t+\Delta T} \partial_{t'}\theta_k\,\mathrm{d}t' = & \qquad (6)\\ & \sum_{n=1}^{\Delta T/\Delta t}\left(\int_{t+(n-1)\Delta t}^{t+n\Delta t}\left[-e_{\theta}(\theta_k,y_0,l)+\kappa\partial^2_{x_k}\theta_k-F_{\mathbf{u}\to\theta}(u_{k,2})\right]\mathrm{d}t'\right)\\ & +\sum_{n=1}^{\Delta T/\Delta t}\left(\int_{t+(n-1)\Delta t}^{t+n\Delta t}\left[-\partial_{x_k}(\bar{u}_{k,k}\theta_k)\right]\mathrm{d}t'\right)\\ & +\int_t^{t+\Delta T}\left[-\partial_{X_i}(\bar{u}_{k,i}\theta_k)-\partial_{X_j}(\bar{u}_{k,j}\theta_k)\right]\mathrm{d}t'\end{aligned}$$

with the LES-scale pressure $\bar{P}$ and the temporal averaged velocities

$$\bar{u}_{k,i}=\begin{cases}\dfrac{1}{\Delta T}\displaystyle\int_{t-\Delta T}^{t}u_{k,i}\,\mathrm{d}t, & \text{if } i\neq k\\ \bar{u}_{k,k}(0)-\displaystyle\int_0^{x_k}\left(\partial_{X_j}\left(\bar{u}_{k,j}\right)+\partial_{X_l}\left(\bar{u}_{k,l}\right)\right)\,\mathrm{d}x_k, & \text{else}\end{cases} \qquad (7)$$

An additional model parameter L_{max} limits the eddy size l.

All advective fluxes are calculated using a first order upwind scheme and for the diffusive fluxes a second order central scheme respectively.

Please note that the velocity component in the ODT line direction $u_{k,k}$ is not defined in the ODTLES approach but its time averaged counterpart $\bar{u}_{k,k}$ is defined via eq. (7). On the LES-scale 3D control volumes (see fig. 2 (a)) we solve a pressure Poisson equation to ensure the divergence constraint on the velocity field

$$\sum_{i=1}^{3}\partial_{X_i}\bar{U}_i=0 \qquad (8)$$

where the LES-scale velocities $\bar{U}_i$ are calculated via spatial averaging

$$\bar{U}_i=\sum_{k=1}^{3}\left((1-\delta_{ki})\frac{W(u_{k,i})}{\Delta X_k}\int_{+\frac{\Delta X_k}{2}}^{-\frac{\Delta X_k}{2}}\bar{u}_{k,i}\mathrm{d}t\right) \qquad (9)$$

with the Kronecker symbol δ_{ki}. The weighting function $W(u_{k,i})$ couples the ODT line domains. The simplest choice, used by Gonzalez-Juez *et al.* (2011) is $W(u_{k,i})=0.5$. We are using

$$W(u_{k,i})=\frac{u^{RMS}_{k,i}}{\sum_{l=1}^{3}(1-\delta_{li})u^{RMS}_{l,i}} \qquad (10)$$

Due to this choice of $W(u_{k,i})$ especially in 3D control volumes near walls, the ODT lines perpendicular to the wall are weighted higher. This helps to maintain small scale properties in near-wall flow. For a detailed description of the pressure Poisson equation leading to terms in eq. (5) we refer to Schmidt *et al.* (2008).

CHANNEL FLOW

Due to the simple geometry and fundamental nature of the fully developed turbulent channel flow DNSs have been done (e.g. by Moser *et al.* (1999) and references within) to yield insights into statistical and structural characteristics of wall-bounded flows. There are also investigations of the convective heat transfer between a turbulent fluid and the wall of a channel (e.g. Kawamura *et al.* (1999) and references within). Also ODT (e.g. Kerstein (1999)) and ODTLES (e.g. Gonzalez-Juez *et al.* (2011)) can produce flow profiles and turbulent budget terms in very good agreement with DNSs for the turbulent channel case.

In this section we compare the to DNS of a heated channel within the database of Kawamura (2013) with ODTLES (see section ODTLES) , an adaptive ODT (denoted AODT) version (by Lignell *et al.* (2012)) , and ODT (see section One-Dimensional-Turbulence Model) for a Reynolds number $Re_\tau=395$ (based on the channel half-width h and the friction velocity u_τ) and for Prandtl numbers $Pr=\{0.025,0.71,2\}$. The fluid in the channel (see fig. 1 on the right) is assumed to be heated by a uniform heat flux q_W from both walls leading to a linearly increasing so-called mixed mean temperature $\langle\bar{T}_m\rangle$ whereby the dimensionless temperature is

$$T(\mathbf{x}) = \underbrace{\frac{\mathrm{d}\langle \bar{T}_m \rangle}{\mathrm{d}x_1}}_{=1/\int_A \bar{u}_1 \mathrm{d}A} x_1 + \theta(\mathbf{x}) \tag{11}$$

where $\mathrm{d}A = \mathrm{d}y\mathrm{d}z$ is the cross-sectional area. This leads to the ODTLES time evolutions equations (5) and (6) (eq. (1) for ODT) with the scalar forcing term

$$F_{\mathbf{u}\to\theta}(u_{k,1}) = \frac{u_{2,1}}{\int_A u_{2,1}\mathrm{d}A}\delta_{k,2} \tag{12}$$

For further details especially a more detailed derivation of the forcing term $F_{\mathbf{u}\to\theta}$ we refer to Kawamura *et al.* (1999).

The ODTLES domain for $Pr = \{0.025, 0.71\}$ consists of $N_{LES} = 16$ LES cells and $N_{ODT} = 512$ ODT wafers, but $N_{LES} = 16$ and $N_{ODT} = 1024$ for $Pr = 2$. The ODT results are produced with the ODTLES resolution N_{ODT} for the respective cases.

The model parameters for ODTLES, ODT, and AODT are chosen to be $C = 6.35$, $Z = 392$ and the ODTLES specific parameter $L_{max} = 2$. Please note that the parameters C and Z are optimized for ODT, not ODTLES. The mean velocity profile (see fig. 4(a)) and the streamwise and spanwise velocity RMS (see fig. 4(b)) are shown for the DNS (by Kawamura (2013)), ODTLES, ODT, and AODT for $Re_\tau = 395$.The budget terms of the kinetic energy are shown in fig. 5.

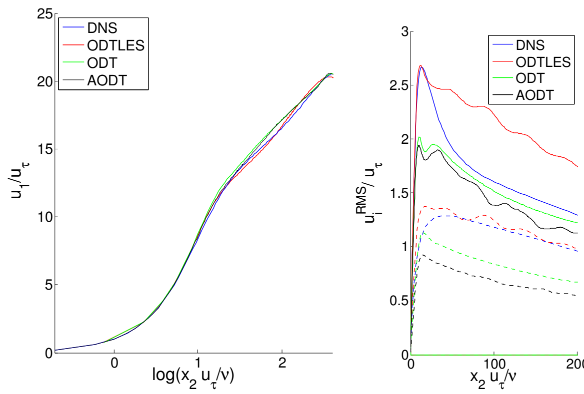

(a) (b)

Figure 4. Streamwise velocity u_1 and streamwise and spanwise velocity RMS u_1^{RMS}(solid) and u_3^{RMS}(dashed) over x_2 in wall coordinates. For ODTLES we use the notation $u_i := u_{2,i}$; $i = \{1,3\}$

The underestimation of the velocity root mean square (from here RMS) at the wall by ODT is a known behavior. ODTLES also dows this. As investigated by Gonzalez-Juez *et al.* (2011) the oscillatory behavior of $u_{2,i}^{RMS}$; $i = \{1,3\}$ is caused by the coupling (see eq. (9)) and decreases for higher N_{LES}. It seems the introduction of the weighting function (eq. (10)) tends to reduce this oscillatory phenomenon in the LES cells near the wall. Further investigation and improvements of the ODTLES coupling are advisable.

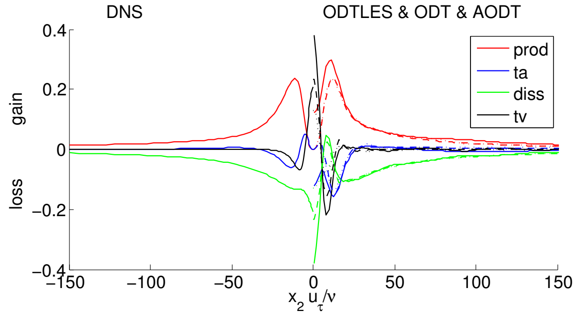

Figure 5. Budget terms of the kinetic energy. The production (prod), turbulent diffusion (tv) and Dissipation (diss) are compared for DNS (at $x_2 < 0$) and (at $x_2 > 0$): ODTLES(solid), ODT(dashed), and AODT(dotted)

The scalar distribution (see fig. 6(a)) and its corresponding RMS (see fig. 6(b)) are also shown for the discussed approaches (DNS,ODTLES,ODT,AODT). The

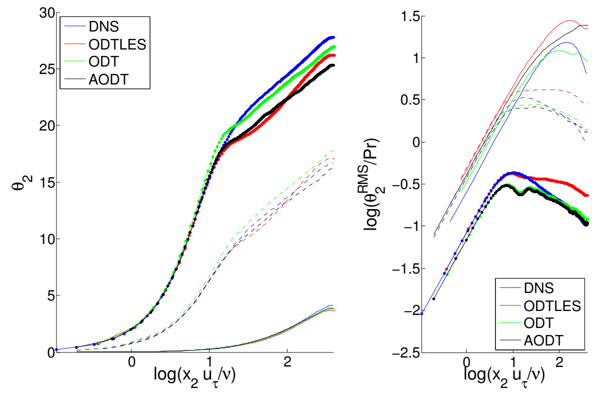

(a) (b)

Figure 6. Scalar mean and RMS profiles for $Pr = 2$ (dashed-dotted), $Pr = 0.71$ (dashed) and $Pr = 0.025$ (solid) vs. x_2 in wall coordinates

scalar distribution as well as its RMS is well represented by ODTLES, ODT, and AODT. The budget terms of the scalar property $(\theta')^2/2$ are shown in fig. 7.

Square Duct Flow

Due to the simple geometry and the secondary flow, DNSs have been done (e.g. Pinelli *et al.* (2010)) to investigate the appearance and behavior of these instabilities. Turbulent fluctuations are inducing these secondary motions. Gonzalez-Juez *et al.* (2011) showed that ODTLES is able to describe the kinematics of the square duct flow with developed secondary instabilities. In this section we study the ODTLES behavior for various Reynolds numbers. ODTLES results for $Re_B = \{1500, 2200, 3500\}$ are compared to DNS (by Uhlmann (2013)). $\{N_{LES}, N_{ODT}\}$ are $\{16, 512\}$, $\{32, 512\}$, and $\{32, 1024\}$ for $Re_B = 1500$, 2200, and 3500 respectively. The ODTLES model parameters $C = 6.35$, $Z = 392$ and $L_{max} = 2$ are chosen to be equal to the heated channel flow case.

First, we compare the streamwise velocity and its RMS (see fig. 8) and the lateral velocity and its RMS

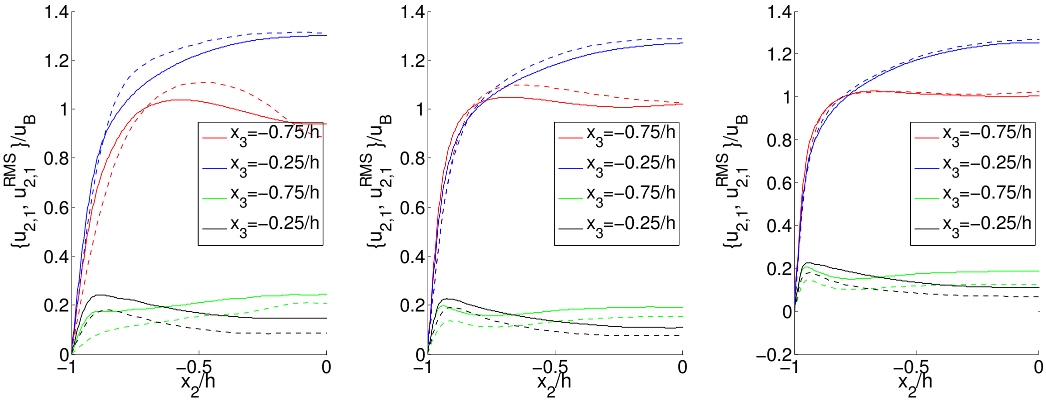

(a) $Re_B = 1500$ (b) $Re_B = 2200$ (c) $Re_B = 3500$

Figure 8. ODTLES results (solid) for the mean (blue and red) and RMS (green and black) streamwise velocity compared to DNS results (dashed) for several sections (see color legend)

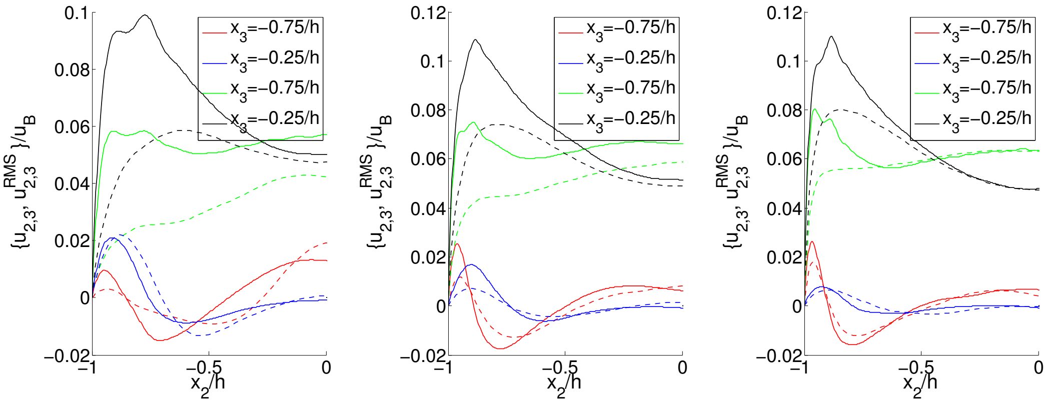

(a) $Re_B = 1500$ (b) $Re_B = 2200$ (c) $Re_B = 3500$

Figure 9. Mean and RMS lateral velocity. Meanings of the lines and colors are same as in fig. 8

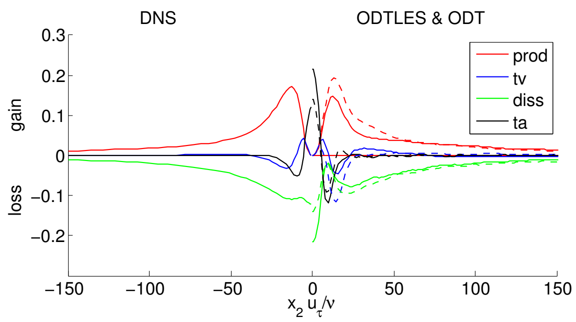

Figure 7. Budget terms of the scalar $(\theta')^2/2$ for $Pr = 0.71$. Meanings of the lines and colors are same as in fig. 5

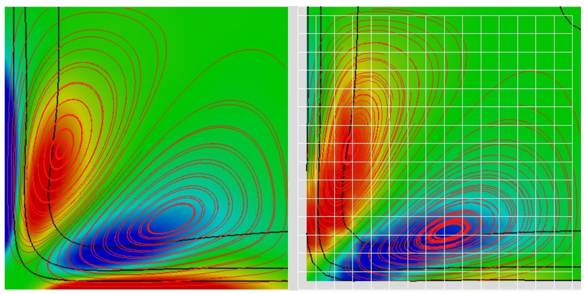

Figure 10. Contour lines $\langle \bar{U}_1 \rangle_{x_1}$ (black), streamlines of the secondary mean flow $(\langle \bar{U}_2 \rangle_{x_1}, \langle \bar{U}_3 \rangle_{x_1})$ (red) and vorticity $\omega_{2D} = \partial_{x_3} \langle \bar{U}_2 \rangle_{x_1} - \partial_{x_2} \langle \bar{U}_3 \rangle_{x_1}$ (RGB color coded) for $Re_B = 2200$ compared to DNS (left). The LES grid (ΔX) is indicated by white lines. All ODTLES quantities are illustrated like cell centered and averaged over all quadrants

(see fig. 9) at certain sections $z/h \approx \{-0.25, 0.75\}$ with DNS (by Uhlmann (2013)) for the three Reynolds numbers. ODTLES primary and secondary flows are both in good agreement with DNS results. The agreement improves with increasing Reynolds number, as observed occasionally using ODT results, because ODT is especially developed to describe turbulent flows. In fig. 10 the LES-scale spatially filtered secondary mean flow is found to be in good agreement with DNS, confirming the results shown in fig. 8 and fig. 9. The LES-scale resolved near-wall flow differs from the DNS because the LES resolution is not able to resolve near-wall effects. In fig. 11 the time-averaged ODT wall-normal-resolved flow is shown to be capable of resolving the near-wall flow in the ODT-resolved direction while also capturing the salient features of the interior flow. For increasing Reynolds numbers the secondary instabilities move towards the corner leading to changes in velocity orientations on smaller spatial scales. ODTLES is capable of resolving this phenomenon with $N_{LES} = 32$ LES cells at least up to $Re_B = 3500$. Main features of the mean wall shear behavior with respect to the Reynolds number

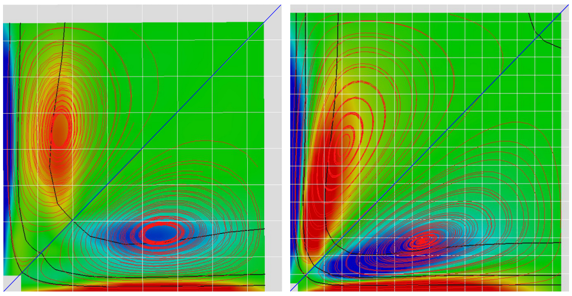

(a) $N_{LES} = 16$ (b) $N_{LES} = 32$

Figure 11. ODT wall-normal-resolved results, using ODT domains resolved in vertically x_2-direction (horizontally x_3-direction) in the lower right (upper left) triangular region for $Re_B = 2200$ compared for different LES resolutions. The meaning of the lines and colors are the same as in fig. 10

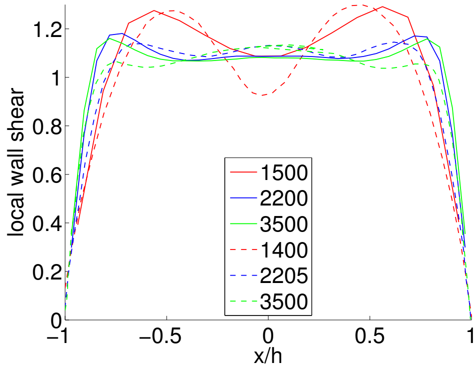

Figure 12. Mean local wall shear $\nu(\sum_{k=2}^{3}(\partial_{x_k}\langle u_{k,1}|_{(x_k=-h)}\rangle_{x_1} - \partial_{x_k}\langle u_{k,1}|_{(x_k=h)}\rangle_{x_1}))/\tau_W$ comparison of DNS results (dashed) and ODTLES results (solid) at different Re_B (see color legend)

(described in detail by Pinelli *et al.* (2010)) can be captured with ODTLES. The extrema flatten with increasing Reynolds numbers and the number of extrema increases.

CONCLUSION

In heated channel flows ODTLES and the (A)ODT implementations agree well, showing that the underlying turbulent fluxes produced by (A)ODT in ODTLES do not degrade due to the 3D ODT domain coupling. Optimizing the model parameters C and Z in ODTLES will further improve the agreement. The introduction of weighting functions into this coupling decreases oscillatory effects in the velocity variations near the wall. The secondary instabilities occuring in the investigated duct flow are resolved including their behavior with respect to the Reynolds number, while ODT is not capable of capturing these 3D effects. While the ODTLES duct results approach DNS results for increasing Reynolds numbers an investigation of high Reynolds numbers $Re_B > 3500$ is of interest for future work. An extension of the scalar properties θ_2 to all ODT line domains $\theta_k, k = \{1,2,3\}$ will allow investigation of e.g. heated ducts (investigated e.g. by Yang *et al.* (2009)) and heated cavities. ODT models are used to investigate buoyant problems (e.g. Wunsch & Kerstein (2000)). Introduction of buoyancy into ODTLES will extend the range of applications to atmospheric flows.

REFERENCES

Ashurst, W. T. & Kerstein, A. R. 2005 One-dimensional turbulence: Variable-density formulation and application to mixing layers. *Physics of Fluids* **17** (2), 025107.

Gonzalez-Juez, E. D., Schmidt, R. C. & Kerstein, A. R. 2011 ODTLES simulation of wall-bounded turbulent flows. *Physics of Fluids* **23** (12), 125102.

Hirota, M., Fujita, H., Yokosawa, H., Nakai, H. & Itoh, H. 1997 Turbulent heat transfer in a square duct. *International Journal of Heat and Fluid Flow* **18**, 170–180.

Kawamura, H. 2013 DNS database. `http://murasun.me.noda.tus.ac.jp/turbulence/index.html`, [Online; accessed Feb 2013].

Kawamura, H., Abe, H. & Matsuo, Y. 1999 DNS of turbulent heat transfer in channel flow with respect to Reynolds and Prandtl number effects. *International Journal of Heat and Fluid Flow* **20**, 196–207.

Kerstein, A. R. 1999 One-dimensional turbulence: Model formulation and application to homogeneous turbulence, shear flows, and buoyant stratified flows. *Journal of Fluid Mechanics* **392**, 277–334.

Kerstein, A. R., Ashurst, W. T., Wunsch, S. & Nilsen, V. 2001 One-dimensional turbulence: Vector formulation and application to free shear flows. *Journal of Fluid Mechanics* **447**, 85–109.

Lignell, D.O., Kerstein, A.R., Sun, G., Monson, E. I., Kerstein, D O Lignell A R & Monson, G Sun E I 2012 Mesh adaption for e cient multiscale implementation of One-Dimensional Turbulence. *Theoretical and Computational Fluid Dynamics* .

Moser, R. D., Kim, J. & Mansour, N. N. 1999 Direct numerical simulation of turbulent channel flow up to $Re_\tau =$ 590. *Physics of Fluids* **11** (4), 943–945.

Pinelli, Alfredo, Uhlmann, Markus, Sekimoto, Atsushi & Kawahara, Genta 2010 Reynolds number dependence of mean flow structure in square duct turbulence. *Journal of Fluid Mechanics* **644**, 107–122.

Piomelli, Ugo, Cabot, William H., Moin, Parviz & Lee, Sangsan 1991 Subgrid-scale backscatter in turbulent and transitional flows. *Physics of Fluids A: Fluid Dynamics* **3** (7), 1766–1771.

Schmidt, H., Kerstein, A. R., Wunsch, S., Nédélec, R. & Sayler, B. J. 2012 Analysis and numerical simulation of a laboratory analog of radiatively induced cloud-top entrainment. *Theoretical and Computational Fluid Dynamics* .

Schmidt, R. C., Kerstein, A. R. & McDermott, R. 2008 ODTLES: A multi-scale model for 3D turbulent flow based on one-dimensional turbulence modeling. *Comput. Methods Appl. Mech. Engrg.* **199** (13–16), 865–880.

Uhlmann, Markus 2013 DNS database. `www.ifh.kit.edu/dns_data`, [Online; accessed Feb 2013].

Wunsch, S. & Kerstein, A. R. 2000 A model for layer formulation in stably stratified turbulence. *Physics of Fluids* **13** (3), 702–712.

Yang, Hongxing, Chen, Tingyao & Zhu, Zuojin 2009 Numerical study of forced turbulent heat convection in a straight square duct. *International Journal of Heat and Mass Transfer* **52** (13-14), 3128–3136.